

Marquette University

e-Publications@Marquette

Biomedical Engineering Faculty Research and Publications

Biomedical Engineering, Department of

10-2015

Fellow Eye Changes in Patients with Nonischemic Central Retinal Vein Occlusion: Assessment of Perfused Foveal Microvascular Density and Identification of Nonperfused Capillaries

Alexander Pinhas

Icahn School of Medicine at Mount Sinai

Michael Dubow

New York Icahn School of Medicine at Mount Sinai

Nishit Shah

New York Eye and Ear Infirmary

Eric Cheang

New York Eye and Ear Infirmary

Chun L. Liu

New York Eye and Ear Infirmary of Mount Sinai

See next page for additional authors

Follow this and additional works at: https://epublications.marquette.edu/bioengin_fac



Part of the [Biomedical Engineering and Bioengineering Commons](#)

Recommended Citation

Pinhas, Alexander; Dubow, Michael; Shah, Nishit; Cheang, Eric; Liu, Chun L.; Razeen, Moataz; Gan, Alexander; Weitz, Rishard; Sulai, Yusufu N.; Chui, Toco Y.P.; Dubra, Alfredo; and Rosen, Richard B., "Fellow Eye Changes in Patients with Nonischemic Central Retinal Vein Occlusion: Assessment of Perfused Foveal Microvascular Density and Identification of Nonperfused Capillaries" (2015). *Biomedical Engineering Faculty Research and Publications*. 418.

https://epublications.marquette.edu/bioengin_fac/418

Authors

Alexander Pinhas, Michael Dubow, Nishit Shah, Eric Cheang, Chun L. Liu, Moataz Razeen, Alexander Gan, Rishard Weitz, Yusufu N. Sulai, Toco Y.P. Chui, Alfredo Dubra, and Richard B. Rosen

Fellow Eye Changes in Patients with Nonischemic Central Retinal Vein Occlusion: Assessment of Perfused Foveal Microvascular Density and Identification of Nonperfused Capillaries

Alexander Pinhas

*Department of Ophthalmology,
New York Eye and Ear Infirmary of Mount Sinai,
Icahn School of Medicine at Mount Sinai,
New York, NY*

Michael Dubow

*Department of Ophthalmology,
New York Eye and Ear Infirmary of Mount Sinai,
Icahn School of Medicine at Mount Sinai,
New York, NY*

Nishit Shah

*Department of Ophthalmology,
New York Eye and Ear Infirmary of Mount Sinai,
New York, NY*

Eric Cheang

*Department of Ophthalmology,
New York Eye and Ear Infirmary of Mount Sinai,
Stuyvesant High School,
New York, NY*

Chun L. Liu

*Department of Ophthalmology,
New York Eye and Ear Infirmary of Mount Sinai,
New York, NY
Bronx High School of Science,
Bronx, New York*

Moataz Razeen

*Department of Ophthalmology,
New York Eye and Ear Infirmary of Mount Sinai,
New York, NY
Alexandria Faculty of Medicine, University of Alexandria,
Alexandria, Egypt*

Alexander Gan

*Department of Ophthalmology,
New York Eye and Ear Infirmary of Mount Sinai,
New York, NY*

Rishard Weitz

*Department of Ophthalmology,
New York Eye and Ear Infirmary of Mount Sinai,
New York, NY*

Yusufu N. Sulai

*The Institute of Optics, University of Rochester,
Rochester, NY*

Toco Y. Chui

*Department of Ophthalmology,
New York Eye and Ear Infirmary of Mount Sinai,
Icahn School of Medicine at Mount Sinai,
New York, NY*

Alfredo Dubra

*Stuyvesant High School,
Department of Biomedical Engineering, Marquette University,
Department of Biophysics, Medical College of Wisconsin,
Milwaukee, WI*

Richard B. Rosen

*Department of Ophthalmology,
New York Eye and Ear Infirmary of Mount Sinai,
Icahn School of Medicine at Mount Sinai,
New York, NY*

Abstract

Purpose: Eyes fellow to nonischemic central retinal vein occlusion (CRVO) were examined for abnormalities, which might explain their increased risk for future occlusion, using adaptive optics scanning light ophthalmoscope fluorescein angiography.

Methods: Adaptive optics scanning light ophthalmoscope fluorescein angiography foveal microvascular densities were calculated. Nonperfused capillaries adjacent to the foveal avascular zone were identified. Spectral domain optical coherence tomography, ultrawide field fluorescein angiographies, and microperimetry were also performed.

Results: Ten fellow eyes of nine nonischemic CRVO and 1 nonischemic hemi-CRVO subjects and four affected eyes of three nonischemic CRVO and one nonischemic hemi-CRVO subjects were imaged. Ninety percent of fellow eyes and 100% of affected eyes demonstrated at least 1 nonperfused capillary compared with 31% of healthy eyes. Fellow eye microvascular density ($35 \pm 3.6 \text{ mm}^{-1}$) was significantly higher than that of affected eyes ($25 \pm 5.2 \text{ mm}^{-1}$) and significantly lower than that of healthy eyes ($42 \pm 4.2 \text{ mm}^{-1}$). Compared with healthy controls, spectral domain optical coherence tomography thicknesses showed no significant difference, whereas microperimetry and 2/9 ultrawide field fluorescein angiography revealed abnormalities in fellow eyes.

Conclusion: Fellow eye changes detectable on adaptive optics scanning light ophthalmoscope fluorescein angiography reflect subclinical pathology difficult to detect using conventional imaging technologies. These changes may help elucidate the pathogenesis of nonischemic CRVO and help identify eyes at increased risk of future occlusion.

Keywords: adaptive optics, fluorescein angiography, retinal microvasculature, image analysis, central retinal vein occlusion, fellow eye

Central retinal vein occlusion (CRVO) is a significant cause of acquired vision loss with a global prevalence of 0.08%.¹ Although a number of major and minor systemic risk factors have been identified,²⁻⁶ a considerable number of patients with CRVO present without identifiable risk factors. Thus, despite years of research since its first description in 1855,⁷ its pathogenesis remains poorly understood.^{8,9}

Epidemiologic studies have shown that eyes fellow to unilateral CRVO have a significantly increased risk of developing venous occlusion compared with the general population.¹⁰⁻¹² Previous studies have shown that before any occlusion, these fellow eyes are both structurally¹³ and electrophysiologically¹⁴ compromised. These findings suggest that additional study of fellow eyes may elucidate the early pathological changes signaling a future occlusive event.

The purpose of this study was to assess the perfused foveal microvascular density and identify nonperfused capillaries in nonischemic CRVO fellow and affected eyes using adaptive optics scanning light ophthalmoscope fluorescein angiography (AOSLO FA)¹⁵ and to compare the findings with previously published data on 16 healthy controls.¹⁶ Spectral domain optical coherence tomography (SD-OCT), ultrawide field fluorescein angiography (UWFFA), and microperimetry—standard clinical modalities for studying retinal structure and function—were also performed.

Methods

Subject Recruitment

This study followed the tenets of the Declaration of Helsinki and was approved by the New York Eye and Ear Infirmary Institutional Review Board. Written informed consent was obtained from each participant after the nature, and potential risks of the study were explained. Retrospective chart review was performed to identify subjects for imaging. Inclusion criteria included a best-corrected visual acuity (BCVA) of $\geq 20/60$ with good central fixation, pupil dilation of at least 5 mm, normal anterior segment with clear crystalline lens, clear media, and minimal or no inner retinal edema at the fovea as

determined using SD-OCT (Heidelberg Spectralis HRA+OCT; Heidelberg Engineering Inc, Heidelberg, Germany). Ten fellow eyes of 9 nonischemic CRVO and 1 superior nonischemic hemi-CRVO subjects (BCVA \geq 20/25; mean age: 45 years; range: 27–67; Table 1) and 4 affected eyes of 3 nonischemic CRVO and 1 superior nonischemic hemi-CRVO subjects (BCVA \geq 20/25 – 2; mean age: 50 years; range: 39–64; Table 2) were imaged. Medical histories were reviewed and fellow eyes with any preexisting retinopathy were excluded. All subjects underwent a single imaging session. Previously published data from 16 healthy eyes were used for comparison.¹⁶ The 16 healthy adults included 8 men and 8 women with a mean age of 25 years (range: 21–29). They had no significant medical or surgical history with normal ocular examination and intraocular pressures and a BCVA of 20/20 or better in each study eye.

Table 1. Demographic of Nonischemic CRVO fellow Eye Patients

Subject ID	Age and Sex	Medical/Social History	Medications	Family History	Ophthalmic History	Time Since RVO
RR_0161	67-year-old woman	HL, elevated sugars	Lovastatin, Aspirin	Father: HL	CRVO OS	2 years
RR_0182	55-year-old man	None	None	Mother: HL; father: DM, HTN; brother: DM	CRVO OD	1.5 years
RR_0235	39-year-old man	None	None	Mother: DM, HTN, HL; 3/7 siblings: DM	Hemi-CRVO OD	7 months
RR_0239	27-year-old man	0.5 PPD for 5 years, quit 6 years ago.	None	Not taken	CRVO OD	1 week
RR_0273	46-year-old woman	Sedentary lifestyle	None	Both parents: DM	CRVO OD	5.5 years
RR_0289	44-year-old man	Borderline HTN	None	Father: DM	CRVO OD	2 years
RR_0298	33-year-old woman	None	None	None	CRVO OS	4 years
RR_0299	37-year-old woman	Anemia	Iron	Mother: HTN	CRVO OS	1 year
RR_0300	50-year-old woman	Heavy drinking (12–24 beers/week). Quit 1 year ago	Multivitamin	Both parents: DM, HTN; sister: DM	CRVO OS	4 years

DM, diabetes mellitus; HL, hyperlipidemia; HTN, hypertension; PPD, packs per day.

Table 2. Demographic of Nonischemic CRVO Affected Eye Patients

Subject ID	Age and Sex	Medical History	Medications	Family History	Ophthalmic History	Time Since RVO	Treatment History	BCVA-Affected Eye
RR_0149	43-year-old man	None	None	Heart disease	CRVO OD	5 years	IBI × 2; 2 years*	20/25 + 2
RR_0151	64-year-old woman	Bipolar disorder	Valproic acid, Risperidone	None	CRVO OS	1.5 years	IBI × 8; 5 months*	20/20
RR_0182	55-year-old man	None	None	Mother: HL; father: DM, HTN; brother: DM	CRVO OD	1.5 years	IBI × 4; 1 year*	20/25 – 2
RR_0235	39-year-old man	None	None	Mother: DM, HTN, HL; 3/7 siblings: DM	Hemi-CRVO OD	7 months	IBI × 1; 5 months*	20/20

*Elapsed time between last IBI and AOSLO FA.
DM, diabetes mellitus; HL, hyperlipidemia; HTN, hypertension; IBI, intravitreal bevacizumab injection.

Clinical Imaging

Charts of the 10 fellow eyes were reviewed for intraocular pressure readings, measured with either applanation tonometry or Tono-Pen (Tono-Pen XL and AVIA; Reichert Inc, New York, NY) near the date of imaging. Before imaging, mydriasis and cycloplegia were induced using 2.5% phenylephrine hydrochloride ophthalmic solution (Bausch & Lomb Inc, Tampa, FL) and 1% tropicamide ophthalmic solution (Akorn Inc, Lake Forest, IL). Axial lengths were measured in all eyes (IOL Master; Carl Zeiss Meditec AG, Jena, Germany) to size the AOSLO image scale in micrometers per pixel using the Emsley schematic eye model.¹⁷

Spectral domain optical coherence tomography imaging and analysis

Spectral domain optical coherence tomography imaging was performed on each of the 10 fellow eyes, using 12 radial scans at 15° intervals through the center of the fovea. Each scan spanned 20° and was an average of 9 frames. Each radial scan was manually segmented to delineate the inner limiting membrane, outer plexiform layer/outer nuclear layer interface, and the retinal pigment epithelium/choroid interface. A spline algorithm was used to interpolate between sample points marked on the inner limiting membrane, outer plexiform layer/outer nuclear layer interface, and

retinal pigment epithelium/choroid interface to measure the inner retinal thickness and total retinal thickness (TRT). Inner retinal thickness and TRT each represented means of 144 data points per eye—12 data points per SD-OCT radial scan at 250, 350, 450, 550, 650, and 750 μm radial distance from foveal center in both directions, times 12 SD-OCT radial scans through the foveal center per eye. Then, IRT/TRT ratios were calculated per fellow eye and compared with respective previously acquired data from 16 healthy eyes.

Microperimetry

Microperimetry was performed on fellow eyes after AOSLO FA imaging using a Polar 3 pattern of 28 test points, Goldmann Size III stimuli with duration of 200 milliseconds at 1.5-second intervals, and a 4-2 threshold algorithm (OPKO SD-OCT/SLO with add-on Microperimetry module; OPKO, Miami, FL). Previously published data from 169 healthy eyes were used for comparison.¹⁸ The 169 healthy adults included 71 men and 98 women with a mean age of 48 years (range: 21–85). They had no significant medical history with normal ocular examination and intraocular pressures and a BCVA of 20/25 or better in each study eye.

Ultrawide field fluorescein angiography

All UWFFAs were performed with intravenous fluorescein administration. Patient records were reviewed for recently performed UWFFA (Optos, Marlborough, MA) on the fellow eyes (within 3 years of AOSLO FA imaging). Ultrawide field fluorescein angiography was acquired for patients without previous studies. Late-phase UWFFA images of the fellow eyes were assessed by two retina specialists for abnormalities.

Adaptive Optics Scanning Light Ophthalmoscope Fluorescein Angiography Imaging and Analysis

The AOSLO machine was a replica of the one built by Dubra and Sulai,¹⁹ modified for AOSLO FA as described by Pinhas et al.¹⁵ Adaptive optics scanning light ophthalmoscope fluorescein angiography imaging and image processing were performed as described by Pinhas et al.¹⁶

Fluorescein was administered orally for AOSLO FA imaging to allow for a longer imaging window. Simultaneous 1.75° field-of-view infrared (IR) confocal reflectance (790 nm) and fluorescence (488 nm) image sequences were acquired approximately 10 minutes after oral fluorescein administration. The fluorescence channel was focused on the superficial layers of retinal microvasculature, and the IR reflectance channel was focused on the photoreceptors. A square region of approximately 6° × 6° in size centered at the fovea was imaged. A set of images using the IR channel covering a 2.5° × 2.5° region around the fovea focused on the superficial layers of retinal microvasculature was also acquired. All sources were treated as lasers for the purposes of maximum permissible exposure calculations. Light exposure was determined to be 6 times below both the photochemical and thermal maximum permissible exposure limits according to the American National Standards Institute (ANSI) Z136.²⁰

Respective registered averaged images with high signal-to-noise ratio were stitched together to create larger IR structural and FA perfusion maps (Adobe Photoshop CS6; Adobe Systems, Inc, San Jose, CA). Comparison of the IR structural with the FA perfusion maps revealed nonperfused capillaries adjacent to the foveal avascular zone (Figure 1, A and B). Circular FA perfusion maps centered on the fovea with a radius of 800 μm were skeletonized in a semiautomated fashion using a custom-developed MATLAB GUI program (Mathworks, Inc, Natick, MA), as previously described.¹⁶ The skeletonized perfusion maps were then divided into equiangular octants and 8 consecutive annuli with a 100- μm radial step-size, creating 64 regions of interest (Figure 2, A–C). Microvascular density was calculated per region of interest, and individual region of interest values were grouped into annulus, octant, and eye means, which were further averaged per study group. In calculating mean microvascular densities per eye, the central 400 μm was excluded to avoid the effect of substantial foveal avascular zone diameter variation across individuals.

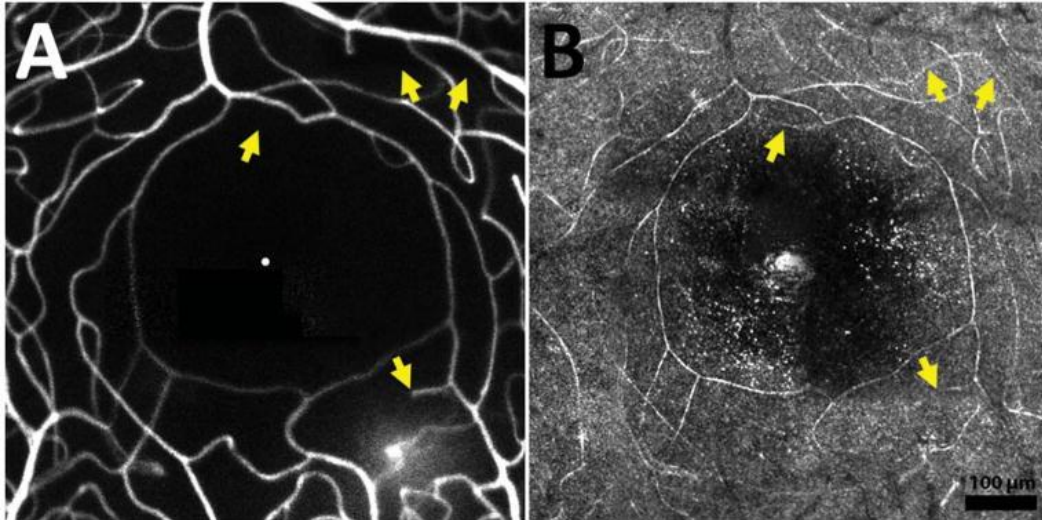


Fig. 1. A. Fluorescein angiography perfusion map of RR_0289 fellow eye (left eye), showing foveal avascular zone and surrounding capillaries. **B.** Corresponding IR structural map. Arrows indicate non-perfused capillaries.

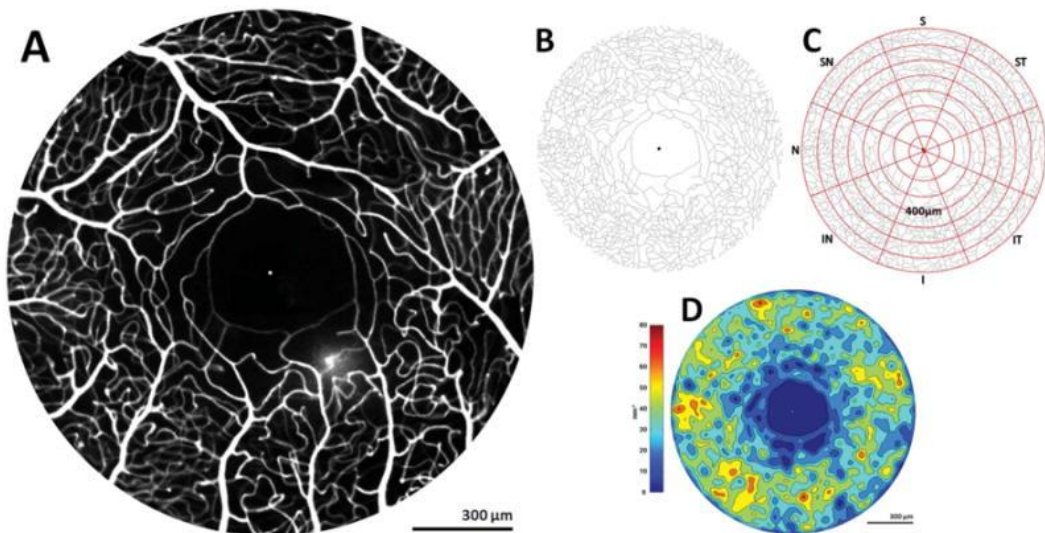


Fig. 2. A. Fluorescein angiography (FA) perfusion map of RR_0289 fellow eye (left eye). **B.** Corresponding skeletonized FA perfusion map with **(C)** octant and annulus grid overlay. **D.** Colored density contour map. S, superior; SN, superior nasal; N, nasal; IN, inferior nasal; I, inferior; IT, inferior temporal; T, temporal; ST, superior temporal.

A separate algorithm created colored density contour maps by computing microvascular density within each $16 \times 16\text{-}\mu\text{m}$ sampling window with $8\text{-}\mu\text{m}$ overlaps over the skeletonized perfusion maps using the built-in MATLAB function `blkproc`. These maps provided a more easily interpretable graphic representation of regional

microvascular density variations across the FA perfusion maps (Figure 2D).

Results

Under the assumption of normally distributed variables, IRT/TRT ratios, microperimetry, and microvascular density group averages \pm SD values were compared for significant differences using an unpaired 2-tailed *t*-test with a *P* value of <0.05 .

All 10 fellow eyes had intraocular pressures ≤ 21 mmHg. Spectral domain optical coherence tomography average IRT/TRT ratio of the 10 fellow eyes was lower than that of healthy eyes; however, this difference was not quite statistically significant (0.37 ± 0.04 vs. 0.39 ± 0.04 ; $t(24) = 1.2$, $P = 0.23$). Microperimetry average sensitivity of the 10 fellow eyes (17 ± 1.4 , range: 12–20 dB) was significantly lower compared with previously reported normative data (18 ± 1.2 , range: 13–20 dB)¹⁸; $t(177) = 2.5$, $P = 0.0120$. Previous records of UWFFA were available for 7 fellow eye patients within 3 years before AOSLO FA imaging, and UWFFA was acquired within 3 months after AOSLO FA for 2 fellow eye patients. RR_0273 was lost to follow-up before we were able to obtain UWFFA images. On assessment, RR_0235 showed leakage at a terminal branch of the superotemporal arcade and RR_0289 showed a few central and peripheral microaneurysms (Figure 3, A and B). Ultrawide field fluorescein angiography was within normal limits for the rest of the 7/9 fellow eyes.

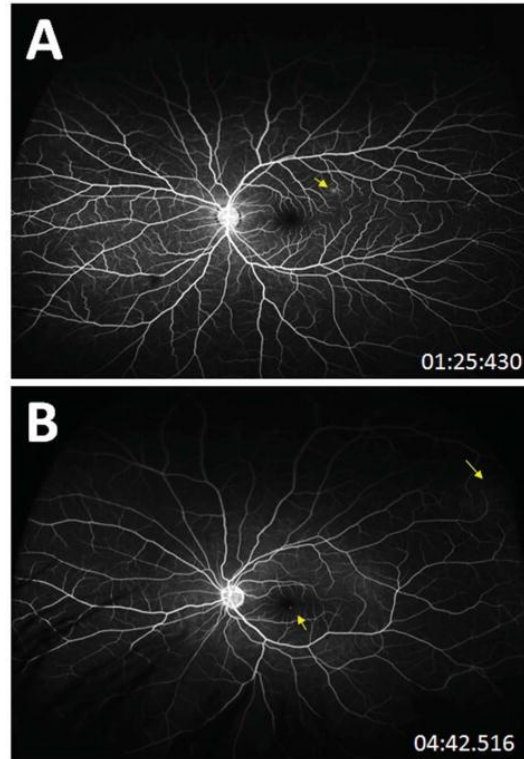


Fig. 3. Examples of fellow eye angiopathy discovered on ultrawide field fluorescein angiography. **A.** RR_0235 left eye showed leakage at a terminal branch of the superotemporal arcade. **B.** RR_0289 left eye showed a few central and peripheral microaneurysms (arrows).

Comparing AOSLO IR structural and FA perfusion maps allowed detection of at least 1 nonperfused capillary segment in 90% of the 10 fellow eyes (Figure 1, A and B) and 100% of the 4 affected eyes, compared with a 31% rate found in the 16 healthy eyes. Average microvascular density \pm SD of the 10 fellow eyes was $35 \pm 3.6 \text{ mm}^{-1}$ (range: 30–41 mm^{-1}), significantly lower than that of the 16 healthy eyes ($42 \pm 4.2 \text{ mm}^{-1}$; range: 33–50 mm^{-1} ; $t(24) = 4.4$, $P = 0.0002$) and significantly higher than that of the 4 nonischemic CRVO-affected eyes ($25 \pm 5.2 \text{ mm}^{-1}$; range: 18–30 mm^{-1} ; $t(12) = 4.2$, $P = 0.0013$) (Table 3; Figure 4, A and B). Figures 5 and 6 are 2 examples of FA perfusion and colorized density contour maps, each showing an affected and fellow eye pair compared with a representative healthy eye. The unaffected octants of the nonischemic hemi-CRVO-affected eye resembled fellow eyes in microvascular density values (Table 2; Figure 6).

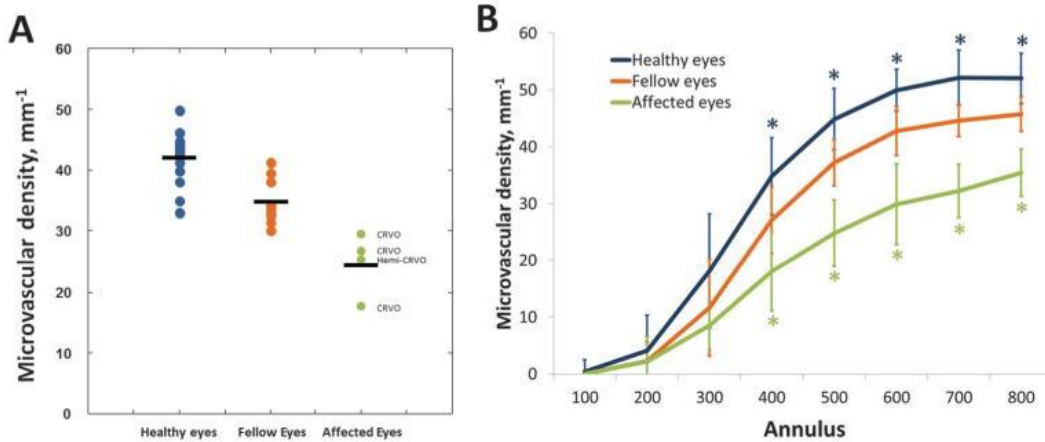


Fig. 4. A. Scatter plot of microvascular density values of fellow eyes ($n = 10$), compared with healthy ($n = 16$) and affected eyes ($n = 4$). Microvascular density values are presented per eye as averages of annuli 300–800. Black bars indicate group averages. **B.** An annulus comparison of microvascular densities of the 3 groups. Error bars represent SD. Asterisks indicate significant differences (unpaired t -test with $P < 0.05$) between healthy and fellow eyes (blue asterisks) and affected and fellow eyes (green asterisks) in microvascular densities at a given annulus.

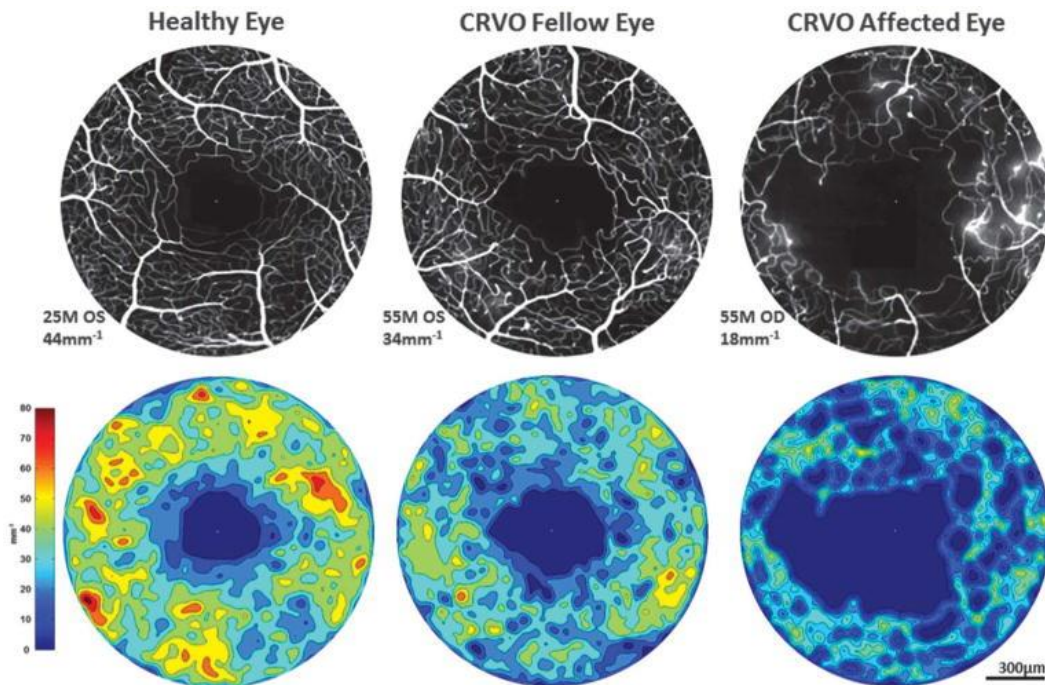


Fig. 5: RR0182-affected eye (nonischemic central retinal vein occlusion in the right eye) and fellow eye (left eye) compared with a healthy control eye, with fluorescein angiography (FA) perfusion maps and corresponding colored density contour maps. Subject age, sex, eye imaged, and perfused foveal microvascular density (mean of annuli 300–800) appear in the lower left corner of respective FA perfusion maps.

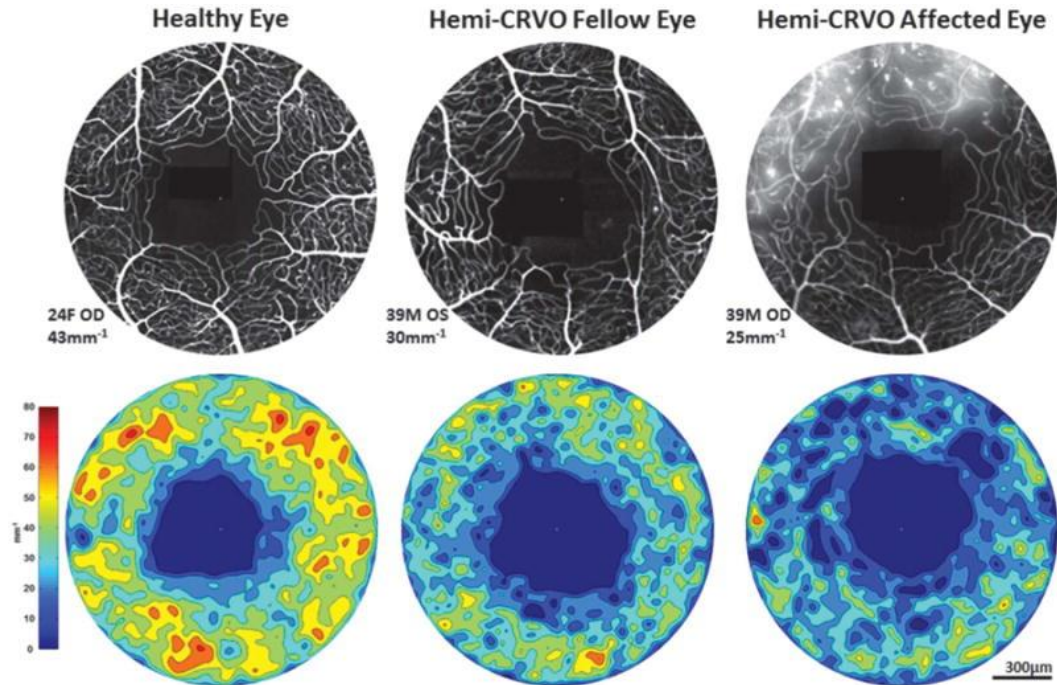


Fig. 6. RR0235-affected eye (nonischemic superior hemiretinal vein occlusion in the right eye) and fellow eye (left eye) compared with a healthy control eye, with fluorescein angiography (FA) perfusion maps and corresponding colorized density contour maps. Subject age, sex, eye imaged, and perfused foveal microvascular density (mean of annuli 300–800) appear in the lower left corner of respective FA perfusion maps.

Table 3. Microvascular Density Results

Eyes	Microvascular Density \pm SD (mm^{-1})
Healthy eyes (n = 16)	42 ± 4.2
Affected eyes (n = 4)	25 ± 5.2
Fellow eyes (n = 10)	35 ± 3.6
Superior hemi-CRVO eye (n = 1)	SN, S, ST 18 IN, I, IT 34

Fellow eye microvascular densities were significantly lower than the 16 healthy eyes and significantly higher than the 4 affected eyes. Unaffected octants of the nonischemic superior hemi-CRVO-affected eye had density values similar to fellow eyes.

I, inferior; IN, inferior nasal; IT, inferior temporal; N, nasal; S, superior; SN, superior nasal; ST, superior temporal; T, temporal.

Discussion

Spectral domain optical coherence tomography average IRT/TRT ratios were not significantly different between healthy and fellow eyes. Seven of nine of the fellow eyes did not have signs of vascular

compromise on UWFFA. Fellow eye sensitivity on microperimetry was on the lower side of normal but remained within clinically acceptable levels. Adaptive optics scanning light ophthalmoscope fluorescein angiography revealed an increased number of non-perfused capillaries near the foveal avascular zone and decreased perfused foveal microvascular density in fellow eyes, compared with healthy data. Microvascular compromise may directly cause previously documented fellow eye structural and functional abnormalities^{13,14}; however, with the current limited data, the sequence of events remains uncertain.

Using current knowledge of pathophysiology, we attempt to explain why eyes fellow to nonischemic CRVO may show decreased foveal microvascular density. The major risk factors for CRVO have been identified as increasing age, hypertension, diabetes, arteriosclerotic vascular risk factors (i.e., hyperlipidemia), and glaucoma.⁹ Although there are marked differences in the pathogenesis of each risk factor, it has been shown that subclinical inflammation with the production of reactive oxygen species is an early shared pathogenic step.²¹⁻³¹ Thus, even before clinically evident disease, inflammation and reactive oxygen species can cause direct damage to the endothelium and lead to capillary closure. Furthermore, the increased expression of adhesion molecules during inflammation causes leukostasis, which can cause physical obstruction of capillary lumens resulting in nonperfusion.³² Dehydration and hypercoagulability disorders, additional CRVO risk factors,⁶ may also lead to capillary nonperfusion. The subclinical nature of these changes preceding clinical disease may explain why the majority of our fellow eye subjects did not report any of the known risk factors for CRVO, yet had a history of nonischemic CRVO in 1 eye and decreased microvascular density in the fellow eye.

Decreased microvascular density observed in fellow eyes may be a predictor of increased risk of future occlusion. The same processes that cause damage to the microvascular endothelium may affect larger vessels, leading to injury accumulation in the central retinal vasculature and ultimately CRVO. Another possibility is an acute-on-chronic mechanism where the chronic subclinical development of capillary non-perfusion leads to local tissue hypoxia and an increase in the production of reactive factors, such as endothelin-1 (vasoconstriction) and vascular endothelial growth factor

(vessel permeability).³³ Fraenkl et al have proposed that elevated concentrations of these factors can lead to the clinical picture of CRVO— a functional constriction of the vein, edema, and hemorrhage.³³

There are some noted limitations of this preliminary study besides the small sample size. Because increasing age is itself a risk factor for CRVO that may cause decreased microvascular density, we believe that it was appropriate to compare nonischemic CRVO fellow eye results with non-age-matched healthy controls in their 20s. However, future studies should include a larger sample size and control for age. Another limitation of this study was that the medical histories collected from all subjects were self-reported. Most of our nonischemic CRVO subjects reported having undergone an extensive workup for the reason of occlusion that was inconclusive. Future studies with larger sample sizes should include a more comprehensive collection of blood pressure history, hemoglobin A1c, and lipid panel trends. Another limitation of this study was that all of the nonischemic CRVO-affected eyes had undergone treatment with intravitreal bevacizumab. This treatment likely slowed or may have even reversed the natural course of microvascular disease, limiting our comparison of affected eye data with fellow and healthy eye data.

There were a few notable limitations in acquisition of conventional images. The fact that a number of the UWFFAs were not performed near the time of AOSLO FA limits any statement of sensitivity of this modality for detecting subclinical pathology. Also, because microperimetry was performed in most cases immediately after AOSLO FA, microperimetry sensitivity may have on average been lower because of temporary bleaching of retina by blue light used in AOSLO FA.

Future prospective studies of the retinal microvasculature may be able to more fully determine the role of these anatomic changes in the pathogenesis of venous occlusion. The ability to study these phenomena at the capillary level over time may provide many additional insights into microvascular changes that have previously been unavailable because of limitations of our clinical imaging tools.

Acknowledgments

The authors thank Richard Bavier for his assistance with AOSLO FA imaging and image processing.

Supported by Marrus Family Foundation, Bendheim–Lowenstein Family Foundation, Wise Family Foundation, RD & Linda Peters Foundation, Edith C. Blum Foundation, Chairman's Research Fund of the New York Eye and Ear Infirmary of Mount Sinai, the Glaucoma Research Foundation, an unrestricted departmental grant from Research to Prevent Blindness, and National Institutes of Health grants P30EY001931 and UL1TR000055. A. Dubra is the recipient of a Career Development Award from Research to Prevent Blindness and a Career Award at the Scientific Interface from the Burroughs Wellcome Fund.

Footnotes

A. Dubra: US Patent No: 8,226,236: Code P (Patent). R. B. Rosen: Clarity: Code C (Consultant); Opticology: Code C (Consultant); OD–OS: Code C (Consultant); Allergan: Code C (Consultant); Carl Zeiss Meditec: Code C (Consultant); Optovue: Code C (Consultant); Advanced Cellular Technologies: Code C (Consultant). The other authors do not have any conflicting interests to disclose.

References

1. Rogers S, McIntosh RL, Cheung N, et al. The prevalence of retinal vein occlusion: pooled data from population studies from the United States, Europe, Asia, and Australia. *Ophthalmology*. 2010;117:313–319
2. Cheung N, Klein R, Wang JJ, et al. Traditional and novel cardiovascular risk factors for retinal vein occlusion: the multiethnic study of atherosclerosis. *Invest Ophthalmol Vis Sci*. 2008;49:4297–4302.
3. Ehlers JP, Fekrat S. Retinal vein occlusion: beyond the acute event. *Surv Ophthalmol*. 2011;56:281–299.
4. Zhou JQ, Xu L, Wang S, et al. The 10-year incidence and risk factors of retinal vein occlusion: the Beijing eye study. *Ophthalmology*. 2013;120:803–808.
5. Jonas JB, Nangia V, Khare A, et al. Prevalence and associations of retinal vein occlusions: the Central India Eye and Medical Study. *Retina*. 2013;33:152–159.
6. Macdonald D. The ABCs of RVO: a review of retinal venous occlusion. *Clin Exp Optom*. 2014;97:311–323.
7. Liebreich R. Apoplexia retinae. *Albrecht von Graefes Arch Ophthalmol*. 1855;1:346.

8. Magargal LE. Venous occlusive disease of the retina. In: Tasman WJ, Edward A, Benson WE, editors. *Duane's Ophthalmology on CD-rom*. Hagerstown, MD: Lippincott Williams & Wilkins Publishers; 2006.
9. McAllister IL. Central retinal vein occlusion: a review. *Clin Exp Ophthalmol*. 2012;40:48–58.
10. McIntosh RL, Rogers SL, Lim L, et al. Natural history of central retinal vein occlusion: an evidence-based systematic review. *Ophthalmology*. 2010;117:1113–1123.
11. Natural history and clinical management of central retinal vein occlusion. The central vein occlusion study group. *Arch Ophthalmol*. 1997;115:486–491.
12. Giuffre G, Randazzo-Papa G, Palumbo C. Central retinal vein occlusion in young people. *Doc Ophthalmol*. 1992;80:127–132.
13. Kim MJ, Woo SJ, Park KH, et al. Retinal nerve fiber layer thickness is decreased in the fellow eyes of patients with unilateral retinal vein occlusion. *Ophthalmology*. 2011;118:706–710.
14. Sakaue H, Katsumi O, Hirose T. Electroretinographic findings in fellow eyes of patients with central retinal vein occlusion. *Arch Ophthalmol*. 1989;107:1459–1462.
15. Pinhas A, Dubow M, Shah N, et al. In vivo imaging of human retinal microvasculature using adaptive optics scanning light ophthalmoscope fluorescein angiography. *Biomed Opt Express*. 2013;4:1305–1317.
16. Pinhas A, Razeen M, Dubow M, et al. Assessment of perfused foveal microvascular density and identification of nonperfused capillaries in healthy and vasculopathic eyes. *Invest Ophthalmol Vis Sci*. 2014;55:8056–8066.
17. Smith G, Atchison DA. *The Eye and Visual Optical Instruments*. Cambridge: Cambridge University Press; 1997.
18. Sabates FN, Vincent RD, Koulen P, et al. Normative data set identifying properties of the macula across age groups: integration of visual function and retinal structure with microperimetry and spectral-domain optical coherence tomography. *Retina*. 2011;31:1294–1302.
19. Dubra A, Sulai Y. Reflective afocal broadband adaptive optics scanning ophthalmoscope. *Biomed Opt Express*. 2011;2:1757–1768.
20. Delori FC, Webb RH, Sliney DH. American National Standards Institute. Maximum permissible exposures for ocular safety (ANSI 2000), with emphasis on ophthalmic devices. *J Opt Soc Am A Opt Image Sci Vis*. 2007;24:1250–1265.
21. Lin CP, Lin FY, Huang PH, et al. Endothelial progenitor cell dysfunction in cardiovascular diseases: role of reactive oxygen species and inflammation. *Biomed Res Int*. 2013;2013:845037.

22. Mittal M, Siddiqui MR, Tran K, et al. Reactive oxygen species in inflammation and tissue injury. *Antioxid Redox Signal*. 2014;20:1126–1167.
23. Czypiorski P, Rabanter LL, Altschmied J, et al. Redox balance in the aged endothelium. *Z Gerontol Geriatr*. 2013;46:635–638.
24. Viridis A, Dell'Agnello U, Taddei S. Impact of inflammation on vascular disease in hypertension. *Maturitas*. 2014;78:179–183.
25. Coban E, Nizam I, Topal C, et al. The association of low-grade systemic inflammation with hypertensive retinopathy. *Clin Exp Hypertens*. 2010;32:528–531.
26. Silva KC, Pinto CC, Biswas SK, et al. Hypertension increases retinal inflammation in experimental diabetes: a possible mechanism for aggravation of diabetic retinopathy by hypertension. *Curr Eye Res*. 2007;32:533–541.
27. Mohamed IN, Soliman SA, Alhusban A, et al. Diabetes exacerbates retinal oxidative stress, inflammation, and microvascular degeneration in spontaneously hypertensive rats. *Mol Vis*. 2012;18:1457–1466.
28. Jousen AM, Poulaki V, Le ML, et al. A central role for inflammation in the pathogenesis of diabetic retinopathy. *FASEB J*. 2004;18:1450–1452.
29. Tousoulis D. Inflammation in atherosclerosis: current therapeutic approaches. *Curr Pharm Des*. 2011;17:4087–4088.
30. Siasos G, Tousoulis D, Oikonomou E, et al. Inflammatory markers in hyperlipidemia: from experimental models to clinical practice. *Curr Pharm Des*. 2011;17:4132–4146.
31. Pinazo-Duran MD, Zanon-Moreno V, Garcia-Medina JJ, Gallego-Pinazo R. Evaluation of presumptive biomarkers of oxidative stress, immune response and apoptosis in primary open-angle glaucoma. *Curr Opin Pharmacol*. 2013;13:98–107.
32. Matsuoka M, Ogata N, Minamino K, Matsumura M. Leukostasis and pigment epithelium-derived factor in rat models of diabetic retinopathy. *Mol Vis*. 2007;13:1058–1065.
33. Fraenkl SA, Mozaffarieh M, Flammer J. Retinal vein occlusions: the potential impact of a dysregulation of the retinal veins. *EPMA J*. 2010;1:253–261.